

# Lawrence Berkeley National Laboratory

## Lawrence Berkeley National Laboratory

### Title

Protein-Folding Landscapes in Multi-Chain Systems

### Permalink

<https://escholarship.org/uc/item/4wn2z7wv>

### Authors

Cellmer, Troy  
Bratko, Dusan  
Prausnitz, John M.  
[et al.](#)

### Publication Date

2005-06-20

Peer reviewed

## **Protein-Folding Landscapes in Multi-Chain Systems**

Major Classification: Biological Sciences

Minor Classification: Biophysics

Authors: Troy Cellmer<sup>1</sup>, Dusan Bratko<sup>1,2</sup>, John M. Prausnitz<sup>1,3</sup>, and Harvey Blanch<sup>1,\*</sup>

<sup>1</sup>Department of Chemical Engineering, University of California, Berkeley, CA 94720

<sup>2</sup>Department of Chemistry, Virginia Commonwealth University, Richmond, VA 23284

<sup>3</sup>Chemical Sciences Division, Lawrence Berkeley National Laboratory, Berkeley, CA 94720

\* corresponding author

Tel: 510-642-1387

Fax: 510-643-1228

[blanch@socrates.berkeley.edu](mailto:blanch@socrates.berkeley.edu)

Number of pages: 25

Number of words (abstract): 141

Number of characters (manuscript, figures, tables, equations, all captions): 46686

## **Abstract**

Computational studies of proteins have significantly improved our understanding of protein folding. These studies are normally carried out using chains in isolation. However, in many systems of practical interest, proteins fold in the presence of other molecules. To obtain insight into folding in such situations, we compare the thermodynamics of folding for a Miyazawa-Jernigan model 64-mer in isolation to results obtained in the presence of additional chains. The melting temperature falls as the chain concentration increases. In multi-chain systems, free-energy landscapes for folding show an increased preference for misfolded states. Misfolding is accompanied by an increase in inter-protein interactions; however, near the folding temperature, the transition from folded chains to misfolded and associated chains is entropically driven. A majority of the most probable inter-protein contacts are also native contacts, suggesting that native topology plays a role in early stages of aggregation.

## I. Introduction

Lattice-model proteins have played a key role in developing our understanding of protein folding. These model proteins contain enough detail to capture the essential physics of the folding process, yet are amenable to rigorous calculation of free-energy landscapes used to describe the folding pathway. Such calculations have provided a conceptual solution to the Levinthal Paradox, which ponders the ability of a protein to navigate a vast amount of conformational space to reach its native state on time scales of seconds or less (1),(2),(3). The funnel-like nature of the free-energy landscapes, first calculated from lattice-models, shows that proteins only need to sample a small fraction of conformations to reach the native state. The energetic bias towards the native state exists because native interactions are, on average, more stable than non-native ones. Similar features are observed in folding landscapes generated from experiments, validating results from model calculations (1).

Most computational studies of protein folding have examined a single chain in isolation(4),(5),(6),(7). However, in many systems of practical interest, including *in vivo* folding, proteins fold in crowded environments. In such situations, interactions with other biological molecules compete with the intra-protein interactions that bias a protein's conformation toward its native state. Some biological molecules, such as molecular chaperones, promote folding(8). However, inter-molecular interactions can also induce misfolding and aggregation(9),(10), resulting in loss of protein function(11). Further, protein aggregates can be toxic. Protein association has been linked to more than twenty human diseases, including Alzheimer's, Parkinson's, and Huntington's diseases(12),(13).

We report simulations for systems containing one, two, or four lattice-model 64-mers. This chain length is greater than that in most model studies of multi-chain systems, and correspondingly provides a more realistic surface-area/volume ratio than that for smaller models(14),(15). Free-energy landscapes have been calculated for the folding of chains in isolation and in systems where individual chains may also form inter-molecular interactions. Throughout all simulations, we use a fixed protein sequence. We increase the number of neighbor molecules to monitor association in addition to folding.

## **II. Methods**

### **Protein sequence and potential function**

We use the conventional on-lattice representation (Figure 1). Protein molecules are represented as self-avoiding chains comprised of amino-acid residues (beads on the chain) interacting through a renormalized Miyazawa-Jernigan (MJ) potential(16),(17). MJ potentials are empirically derived: 20 different amino acids are possible. The renormalization of the solvent-solute interactions introduced by Leonhard *et. al.* (16) corrects for some of the inconsistencies resulting from the approximations underlying the original MJ model. Empirical energy scales such as the present one can at best be used to capture qualitative aspects of protein behavior (18),(19). For a detailed description of the potential function the reader is referred to (16). Each chain consists of 64 beads with the following sequence: *KEKSTAGRVASGVLDSVACGVLGDIDTLQ-GSPIAKLKTFYGNKFNDVEASQAHMIRWPNYTLPE* (Fig. 1). Solvent effects are included implicitly in the Hamiltonian. Studies of different sequences suggest that our present conclusions are qualitatively general and not limited to the chosen sequence.

### **Simulation details**

All simulations were of the standard Monte Carlo form and conducted in the canonical (N,V,T) ensemble. Boundary effects are taken into account by applying periodic (Minimum Image) conditions. We use standard simulation moves including; (1)- displacements of either one of the end beads to one of the available four neighboring sites; (2)- corner flips for beads are characterized by a right angle between the directions to both contour neighbors; (3)- crankshaft moves of bead pairs located at the bottom of a U turn. We also allow forward and backward slithering-snake reptation moves(20), as well as translations of entire chains or groups of chains. Moves are attempted at random with *a priori* probabilities specified in ref.(15) where further details of the (N,V,T) simulations are available.

To alleviate problems related to local trapping on a rugged free-energy landscape, we apply a Replica Exchange Monte Carlo simulation technique (REMC)(15). Systems are allowed to swap between adjacent temperature levels with probabilities that preserve canonical (Boltzmann) statistics within each level. Assuming an approximate Arrhenius dependence of first passage times from the local minimum, the chance of escape of a trapped system is significantly improved during the time it spends at an elevated temperature. A temperature swap was attempted after every simulation pass. The attempted exchange of systems  $i$  and  $j$  with energies  $V_i$  and  $V_j$  between temperature levels  $m$  and  $n$ , was accepted with the probability(21)

$$p_s = \min \left\{ 1, \exp \left[ - \left( \frac{1}{k_B T_n} - \frac{1}{k_B T_m} \right) (V_i - V_j) \right] \right\} \quad (1)$$

In most calculations, the number of replicas (and temperature levels) was six, with reduced temperature  $T$  ranging between 1.0 and 1.3, and typical swapping acceptances between 8-30%. Reduced temperature  $T$  is normalized by the reference temperature  $T_o$

such that  $k_B T_o$  represents the energy unit pertinent to our system. The size of the cubic box equals 12, 14, and 16 monomer lengths corresponding to volume fractions of  $\sim 3.7$ , 4.7, and 6.3% in one-, two-, and four-chain systems, respectively. To alleviate finite-size effects, periodic boundary conditions are applied in all directions.

### Weighted Histogram Analysis Method

The Weighted Histogram Analysis Method (WHAM) was used to analyze simulation data(22). WHAM minimizes the error in the density-of-states function, and facilitates the calculation of free-energy surfaces. Using the number of native contacts  $N_{Nat}$  and the number of inter-protein contacts  $N_{Inter}$  as example reaction coordinates, the density-of-states function has the form

$$\Omega(V, N_{Nat}, N_{Inter}) = \frac{\sum_{j=1}^k N_k(V, N_{Nat}, N_{Inter})}{\sum_{j=1}^k n_j \exp(-f_j - \beta_j V)} \quad (2)$$

where  $N_k$  is the number of occurrences for samples with  $(V, N_{Nat}, N_{Inter})$ ,  $f_j = \beta A_j$  where  $A_j$  is the free energy of simulation  $j$  and  $\beta$  is  $1/k_B T$ ,  $k$  is the number of simulations,  $n_j$  is the number of samples from simulation  $j$ . The density of states can then be used to calculate thermodynamic averages (using  $N_{Nat}$  as an example) via

$$\langle N_{Nat} \rangle = \frac{\sum_{V, N_{Nat}, N_{Inter}} (N_{Nat}) * \Omega(V, N_{Nat}, N_{Inter}) \exp(-\beta V)}{\sum_{V, N_{Nat}, N_{Inter}} \Omega(V, N_{Nat}, N_{Inter}) \exp(-\beta V)} \quad (3)$$

Apart from an undetermined constant, free-energy surfaces are calculated via

$$F(N_{Nat}, N_{Inter}) = -k_B T \ln \{ P_\beta(N_{Nat}, N_{Inter}) \} + Const. \quad (4)$$

where  $P_{\beta}(N_{Nat}, N_{Inter})$  is the probability of observing a system with  $(N_{Nat}, N_{Inter})$  at temperature  $T = (k_B\beta)^{-1}$ . A more complete description of the application of the WHAM equations is in ref.(23).

### III. Results

#### Unfolding occurs at lower temperatures in multi-chain systems

Fig. 2 (upper left) shows heat capacities as a function of temperature for one, two, and four-chain systems. In all three cases, a single, strong peak is observed, suggesting a single phase transition. As the number of chains increases, the peak is shifted to lower temperatures. For a one-chain system, the peak occurs at  $T=1.155$ ; for a two-chain system at 1.12; and for a four-chain system at 1.05.

Further insight into the phase-transition data is obtained from plots of the average number of native contacts ( $N_{Nat}$ , Figure 2, upper right), inter-protein contacts ( $N_{Inter}$ , Fig. 2, lower left), and radius of gyration ( $R_g$ , Fig. 2, lower right) as a function of temperature. When multiple chains are present, thermal denaturation takes place at lower temperatures; a result corroborated by findings from more-realistic models(24). For all three cases, the mid-point temperature of unfolding essentially coincides with the heat-capacity-peak temperature. These data show that the heat-capacity peaks are associated with unfolding events. Further, for multi-chain systems, there are sharp increases at the melting temperatures in the number of inter-protein contacts. Thus, the loss of intra-protein interactions, to some extent, is compensated by an increase in (attractive) inter-protein interactions. Finally, the  $R_g$  vs.  $T$  plot indicates that protein unfolding and association are accompanied by chain expansion.

#### Free energy landscapes for folding



Fig. 3 shows free-energy landscapes for chains simulated in isolation (upper left), in the presence of a second chain (upper right), and in the presence of three other chains (lower center). Progress variables are the native energy (per chain) and non-native energy (per chain). Because these two quantities do not explicitly include inter-chain effects, they allow direct comparison of the landscapes. Further, our progress variables are similar to those used in other lattice-model studies(1).

The plots were produced for systems at  $T=1.05$ . At this temperature, chains simulated in isolation populate the native state  $\sim 99\%$  of the time(23). This result is reflected in the landscape for a single chain in isolation that exhibits a funnel-like shape with only a small barrier to folding. When a second chain is present, the landscape is more rugged, and exhibits two local minima with modest free-energy barriers ( $\sim k_B T$ ) that slow progression towards the native state. However, the funnel-like shape of the landscape is retained, and a noticeable bias towards the native state exists. When a chain can interact with three possible partners, the landscape is remarkably different. There is little bias towards the native structure, as chains spend about half the time populating mis-folded states. The barrier separating the misfolded states from the native state is small, roughly  $1.5k_B T$ .

### **Thermodynamics of association**

Fig. 4 shows free-energy contours versus the number of native and inter-protein contacts for two-chain (left) and four-chain systems (right). The data are plotted *at the phase transition temperatures* ( $T=1.12$  for the two-chain system,  $T=1.05$  for the four-chain system).

In the two-chain system, we see two minima of equal (relative) free energy ( $F$ ). The first, found in the region of the diagram corresponding to a large number of native contacts, corresponds to a pair of native chains that interact through surface residues (labeled A). The second corresponds to non-native chains that interact predominantly through residues that are buried in the native state (labeled B). Fig. 5 (left panel) shows the probability distribution of the potential energy for these two states. The pair of native chains populates states with a potential energy much lower than the non-native aggregate, showing that association is entropically driven. Using the average potential energy for each state, and the fact that the free-energy difference between the two states is zero, we estimate that the average entropy difference between the two states is  $(47 \pm 9)k_B$  per chain. This is similar to the entropy difference  $(43 \pm 11)k_B$  between the unfolded and folded states at the phase-transition temperature for chains in isolation.

Fig.4 (upper right) shows free-energy contours for the four-chain system at  $T=1.05$ . Two adjacent minima (labeled D and E) exist with large numbers of native contacts; they represent states where all four chains are native. The third minimum (labeled F) exists at a region in the diagram with a large number of inter-protein contacts, but at a much smaller number of native contacts; this minimum represents an aggregate of misfolded chains. The two minima corresponding to systems of native proteins were grouped together to generate a state of free energy equal to that of the aggregate. As with the two-chain system, in the vicinity of the transition temperature, aggregate states have potential energies significantly higher than those for states corresponding to native proteins (Fig. 5, upper right). However, because of opportunities for inter-protein

interactions with multiple partners, the entropy difference  $(27k_B \pm 6)k_B$  per chain is lower than that in one-chain and two-chain systems.

### **Contacts leading to aggregation**

To obtain a more complete picture of the association process, we have investigated the specific amino-acid residues and residue contacts that contribute most significantly to the protein-protein interaction potential. Despite the increased entropy of the aggregated state, certain amino-acid residues do play an enhanced role in association. The twelve beads listed in Table I, and shown within the context of the native state in Fig. 6, are involved in interactions that (on average) contribute 50% of the inter-protein potential for aggregates in two-chain and four-chain systems. Five of these beads are buried in the native state. This is consistent with the experimental observation that unfolding facilitates aggregation(25),(26),(27),(28).

Tables II and III list the ten most probable inter-protein contacts found in aggregates. In both two-chain and four-chain systems, nine of the ten contacts are also native contacts; this indicates domain-swapping, which has been observed as a mechanism of aggregation in numerous other systems(29),(30),(31),(32),(33).

### **Discussion**

Free-energy landscapes show that the presence of multiple chains can impede the folding process under conditions where the native state is favored for isolated chains. In two-chain systems, the landscape is more rugged, but the bias towards the native state remains. When the number of chains increases to four, the bias is removed, and individual molecules spend equivalent times in native and misfolded conformations. In systems of practical interest, such as *in vivo* folding(12) and inclusion-body protein

refolding(34), such changes in the free-energy landscape have a deleterious effect. If proteins cannot reach their native state, they are generally unable to carry out their biological function. In *in vivo* folding, molecular chaperones(8), are present to ensure that proteins can attain their native state. Insight into chaperone behavior could be obtained if chaperone sequences that return the folding landscape to its natural form were identified.

The origins of the misfolding behavior observed in multi-chain simulations can be attributed to inter-protein interactions. Intra-molecular energy is traded for inter-molecular energy, thus stabilizing misfolded states. However, in the vicinity of the transition temperature, the loss in intra-protein energy is not fully compensated by inter-protein interactions and the process of association is entropically driven. We are unaware of any experimental results that confirm this finding, and it is difficult to imagine the formation of large aggregates such as inclusion bodies or amyloid fibrils accompanied by an increase in protein entropy. Because our Hamiltonian does not explicitly account for hydrogen bonds, it is possible that we underestimate the effect of such interactions, known to be important in the formation of both inclusion bodies and amyloid fibrils(35),(36). Further, because our systems contain a small number of chains, it is possible that for systems with more than four chains, a phase transition from disordered to ordered aggregates could take place. Such behavior has been observed for more detailed models found in ref. (24),(37). A decrease in the entropy gain is indeed observed in our model upon increasing the number of associated chains. However, experimental and computational studies have shown that amorphous aggregates(24),(38) can act as precursors to ordered assemblies of proteins, such as amyloid fibrils. Because such amorphous aggregates lack the apparent order of fibrils, it seems more feasible that their

formation is favored entropically. Thus if an increase in protein entropy is a driving force for aggregation, it is likely that this increase occurs during the early steps of the association process, prior to the formation of a quaternary structure that can be propagated such that ordered aggregation starts to occur *en masse*.

Despite increased disorder characterizing the aggregated state, some amino acids and amino-acid contacts play a persistent role in folding and aggregation. Most of these amino acids are hydrophobic beads normally buried in the native state. This is not surprising, because we observe an increase in inter-protein association upon protein unfolding. Our finding is also in good agreement with experimental data showing that proteins are particularly prone to aggregation when destabilized, and natively-buried, sticky residues become available for residue-residue interactions(27),(26),(25),(28). Further, the majority of the most probable inter-protein contacts are also native contacts. Not surprisingly, these contacts occur between pairs of residues that are strongly interacting. However, while many pairs of the same interaction energy can be formed between chains, there is a significant bias towards amino-acid pairs that are also formed in the native state. As shown in a previous study (11), interprotein contacts between strings of complementary residues tend to form or rupture simultaneously, suggesting that a mechanism akin to pattern recognition can operate both intra- and inter-molecularly. Native topology therefore plays a role in determining which amino acids play a dominant role in association.

In summary, we have extended a common approach to studying protein folding in isolation to investigate protein folding in the presence of multiple chains. This extension

has not only yielded insight into the folding process, but also into misfolding and aggregation.

### **Acknowledgements**

For financial support, the authors are grateful to the National Science Foundation and to the Office for Basic Energy Sciences of the U.S. Department of Energy.

1. Dinner, A. R., Sali, A., Smith, L. J., Dobson, C. M. & Karplus, M. (2000) *Trends Biochem Sci* **25**, 331-9.
2. Karplus, M. (1997) *Fold Des* **2**, S69-75.
3. Onuchic, J. N. & Wolynes, P. G. (2004) *Curr Opin Struct Biol* **14**, 70-5.
4. Dinner, A. R., Sali, A. & Karplus, M. (1996) *Proc Natl Acad Sci U S A* **93**, 8356-61.
5. Dinner, A. R. & Karplus, M. (1999) *J Mol Biol* **292**, 403-19.
6. Li, L., Mirny, L. A. & Shakhnovich, E. I. (2000) *Nat Struct Biol* **7**, 336-42.
7. Schonbrun, J. & Dill, K. A. (2003) *Proc Natl Acad Sci U S A* **100**, 12678-82.
8. Barral, J. M., Broadley, S. A., Schaffar, G. & Hartl, F. U. (2004) *Semin Cell Dev Biol* **15**, 17-29.
9. Gupta, P., Hall, C. K. & Voegler, A. C. (1998) *Protein Sci* **7**, 2642-52.
10. Istrail, S., Schwartz, R. & King, J. (1999) *J Comput Biol* **6**, 143-62.
11. Dobson, C. M. (2004) *Semin Cell Dev Biol* **15**, 3-16.
12. Dobson, C. (2001) *Phil. Trans. R. Soc. London B* **356**, 133-145.
13. Sacchettini, J. C. & Kelly, J. W. (2002) *Nat Rev Drug Discov* **1**, 267-75.
14. Bratko, D. & Blanch, H. W. (2001) *Journal of Chemical Physics* **114**, 561-569.
15. Bratko, D. & Blanch, H. W. (2003) *Journal of Chemical Physics* **118**, 5185-5194.
16. Leonhard, K., Prausnitz, J. M. & Radke, C. J. (2003) *Physical Chemistry Chemical Physics* **5**, 5291-5299.
17. Leonhard, K., Prausnitz, J. M. & Radke, C. J. (2003) *Biophysical Chemistry* **106**, 81-89.
18. Thomas, P. D. & Dill, K. A. (1996) *Proc Natl Acad Sci U S A* **93**, 11628-33.
19. Thomas, P. D. & Dill, K. A. (1996) *J Mol Biol* **257**, 457-69.
20. Wall, F. T. & Mandel, F. (1975) *Journal of Chemical Physics* **63**, 4592-4595.
21. Gront, D., Kolinski, A. & Skolnick, J. (2000) *Journal of Chemical Physics* **113**, 5065-5071.
22. Kumar, S., Bouzida, D., Swendsen, R., Kollman, P. A. & A., R. J. (1992) *Journal of Computational Chemistry* **13**, 1011-1021.
23. Cellmer, T., Bratko, D., Prausnitz, J. M. & Blanch, H. W. (2005) *Journal of Chemical Physics* **122**.
24. Nguyen, H. D. & Hall, C. K. (2004) *Proc Natl Acad Sci U S A* **101**, 16180-5.
25. Chiti, F., Webster, P., Taddei, N., Clark, A., Stefani, M., Ramponi, G. & Dobson, C. (1999) *Proc. Nat. Acad. Sci. USA* **96**, 3590-3594.
26. Chiti, F., Taddei, N., Bucciantini, M., White, P., Ramponi, G. & Dobson, C. M. (2000) *Embo J* **19**, 1441-9.
27. Ramirez-Alvarado, M., Merkel, J. S. & Regan, L. (2000) *Proc Natl Acad Sci U S A* **97**, 8979-84.
28. Zurdo, J., Guijarro, J. I., Jimenez, J. L., Saibil, H. R. & Dobson, C. M. (2001) *J Mol Biol* **311**, 325-40.
29. Clark, L. A. (2005) *Protein Sci* **14**, 653-62.
30. Fawzi, N. L., Chubukov, V., Clark, L. A., Brown, S. & Head-Gordon, T. (2005) *Protein Sci* **14**, 993-1003.
31. Gotte, G., Vottariello, F. & Libonati, M. (2003) *J Biol Chem* **278**, 10763-9.
32. Janowski, R., Kozak, M., Jankowska, E., Grzonka, Z., Grubb, A., Abrahamson, M. & Jaskolski, M. (2001) *Nat Struct Biol* **8**, 316-20.

33. Ding, F., Dokholyan, N. V., Buldyrev, S. V., Stanley, H. E. & Shakhnovich, E. I. (2002) *J Mol Biol* **324**, 851-7.
34. Clark, E. D. (2001) *Curr Opin Biotechnol* **12**, 202-7.
35. Carrio, M., Gonzalez-Montalban, N., Vera, A., Villaverde, A. & Ventura, S. (2005) *J Mol Biol* **347**, 1025-37.
36. Nilsson, M. R. (2004) *Methods* **34**, 151-60.
37. Hall, C. (2005) *Personal Communication*.
38. Serio, T. R., Cashikar, A. G., Kowal, A. S., Sawicki, G. J., Moslehi, J. J., Serpell, L., Arnsdorf, M. F. & Lindquist, S. L. (2000) *Science* **289**, 1317-21.



Table I. Amino acids that, on average, contribute 50% of the inter-protein interaction potential for two and four-chain systems. LES stands for the lowest-energy structure.

<b>Amino Acid</b>	<b>Amino Acid Identity</b>	<b>Buried in LES</b>
1	K	no
2	E	no
22	L	yes
25	I	yes
26	D	no
33	I	yes
35	K	no
37	K	no
54	M	yes
55	I	yes

Table II. Most probable inter-protein contacts found in aggregates for two-chain systems.

<b>Amino Acid</b>	<b>Amino acid</b>	<b>&lt;Occurrences&gt; per snapshot</b>
54M	55I	0.60
54M	57W	0.59
36L	55I	0.30
25I	36L	0.26
33I	54M	0.26
28L	55I	0.26
26D	35K	0.25
55I	62L	0.22
24D	37K	0.21
54M	63P	0.21

Table III. Most probable inter-protein contacts found in aggregates for four-chain systems.

<b>Amino Acid</b>	<b>Amino acid</b>	<b>&lt;Occurrences&gt; per snapshot</b>
26D	35K	2.69
2E	37K	1.99
24D	37K	1.80
1K	24D	1.49
1K	2E	1.42
25L	36I	1.24
55I	62L	1.23
3K	26D	1.15
2E	35K	1.12
54M	55I	1.05

## Figure Captions

Figure 1. Lowest-energy structure of the model protein.

Figure 2. Heat capacities for single-chain (blue), two-chain (red), and four chain systems (green) as functions of temperature (upper left). Average number of native contacts (per chain) for single-chain (blue), two-chain (red), and four-chain systems (green) as functions of temperature (upper right). Average number of inter-protein contacts (per chain) for two-chain (red) and four chain systems (green) as functions of temperature (lower left). Average radius of gyration (per chain): single-chain (blue), two-chain (red), and four chain systems (green) as functions of temperature (lower right).

Figure 3. Free-energy landscapes for one-chain, two-chain, and four-chain systems.  $V_{\text{native}}$  and  $V_{\text{non-native}}$  are the potential energy contributions from intra-protein native and non-native interactions, respectively.

Figure 4. Free-energy contours for a two-chain system at  $T=1.12$ (left). Free-energy contours for a four-chain systems at  $T=1.05$  (right).  $N_{\text{Nat}}$  and  $N_{\text{Inter}}$  are the number of native and inter-protein contacts per chain, respectively. The contours are in increments of  $2k_{\text{B}}T_0$ .

Figure 5. Potential energy distributions (per chain) for a two-chain system at  $T=1.12$  (left) and four-chain system at  $T=1.05$  (right).

Figure 6. Highlighted beads contribute, on average, 50% of the inter-protein interaction potential.

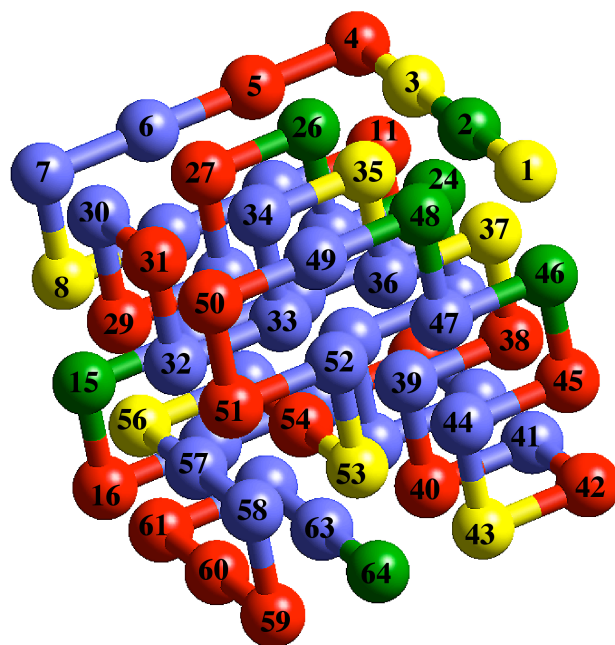


Figure 1

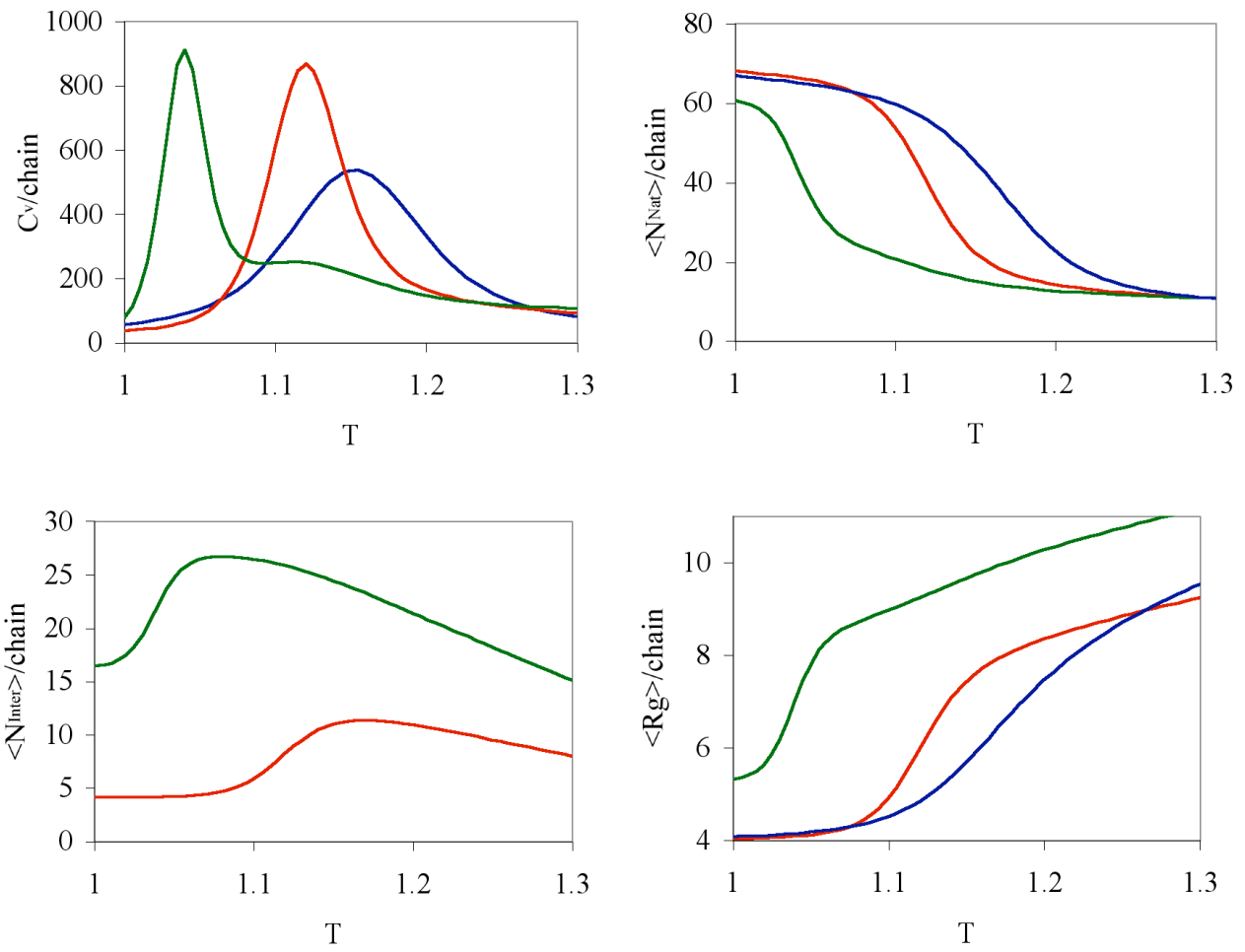


Figure 2

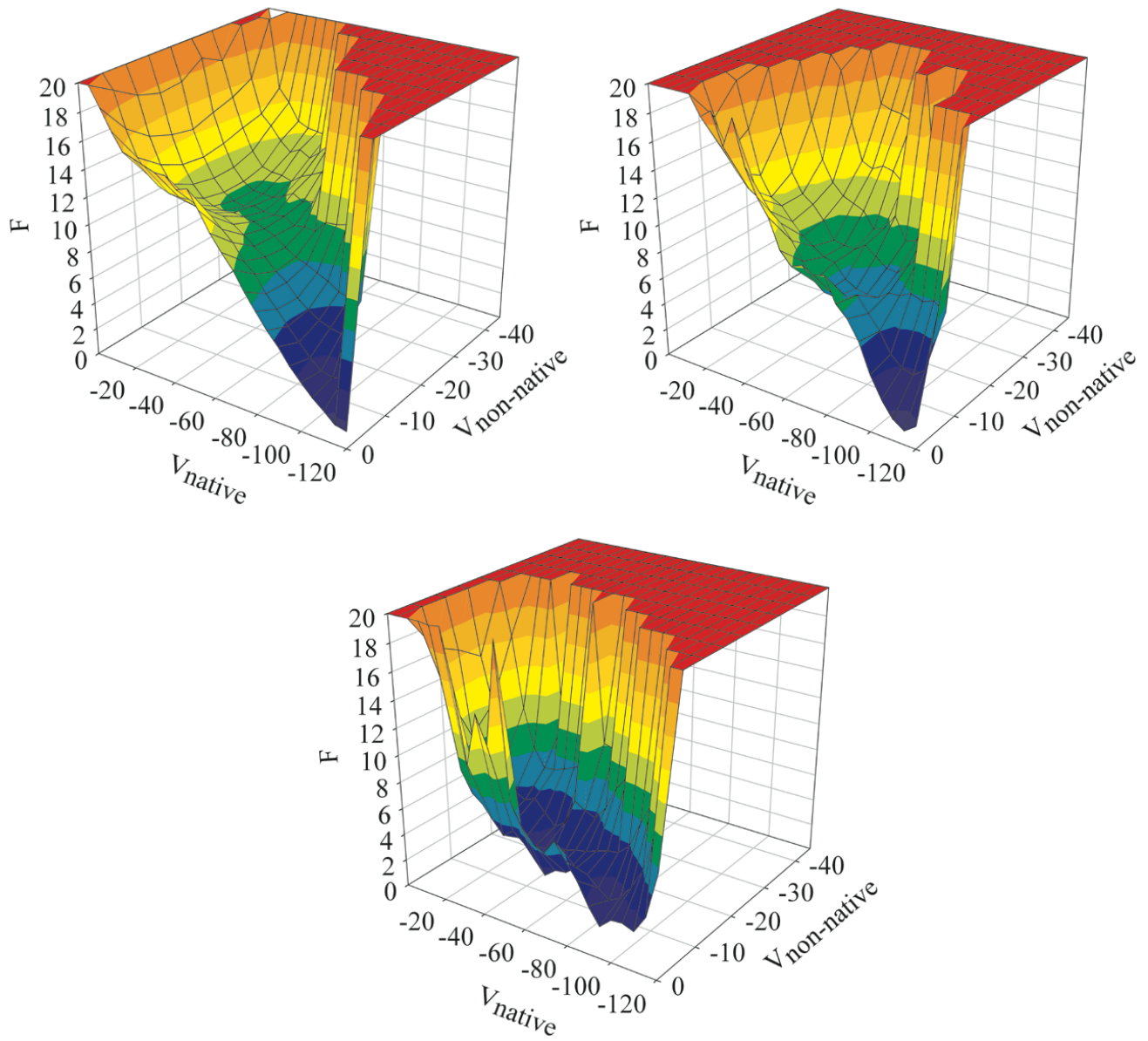


Figure 3

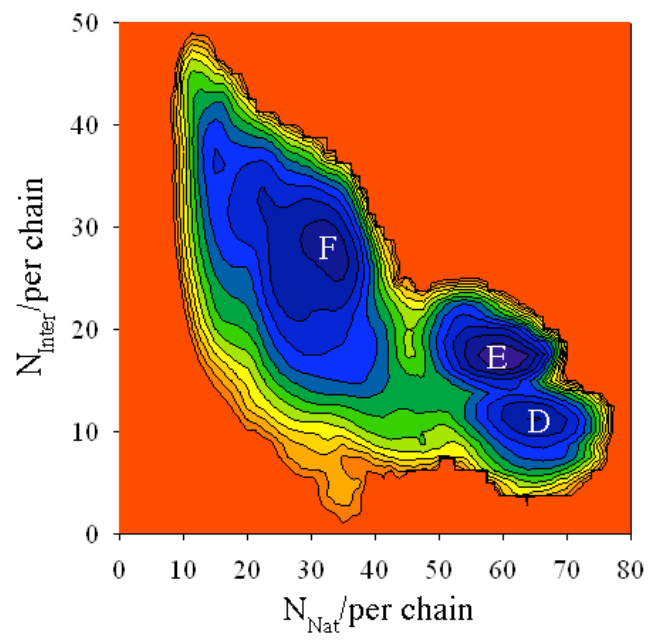
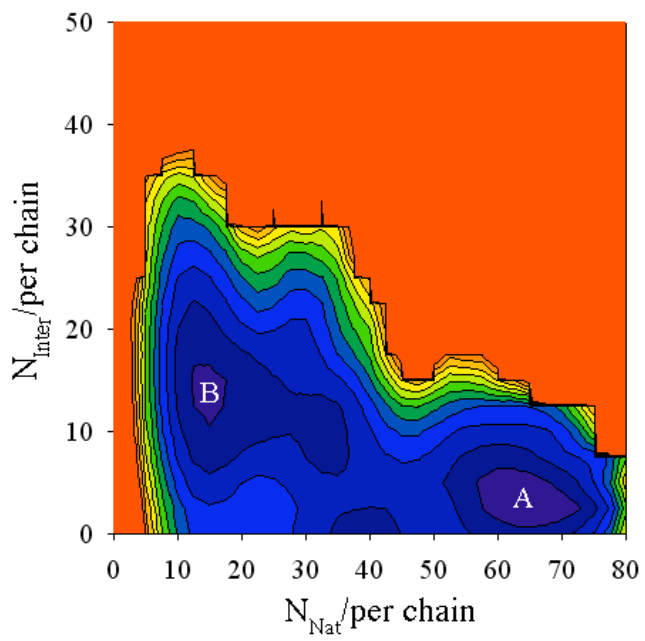


Figure 4



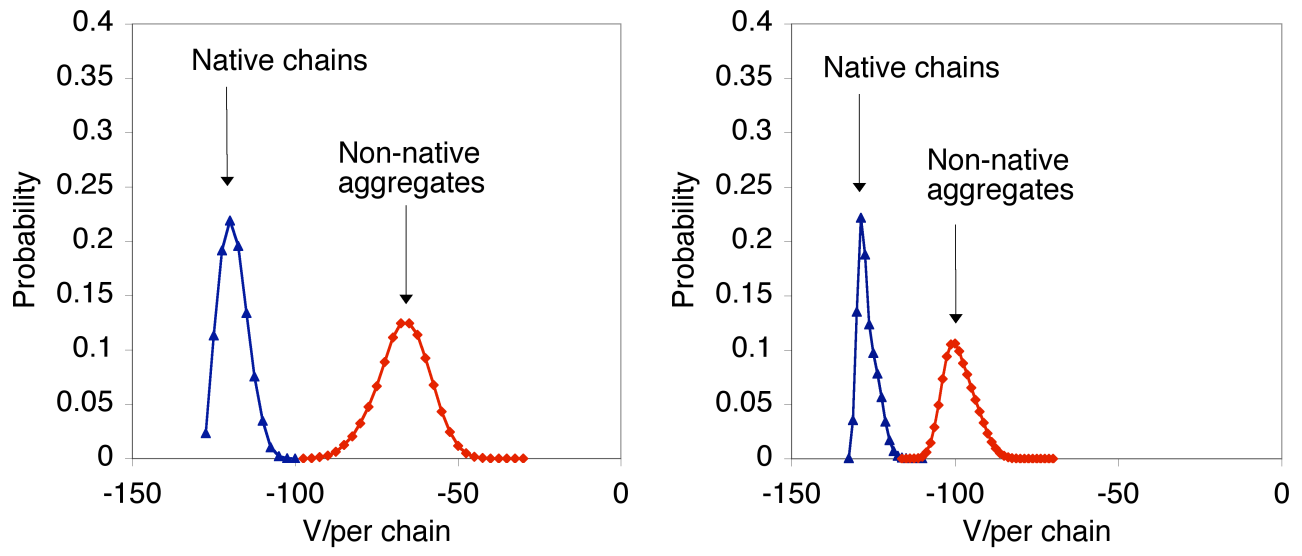


Figure 5

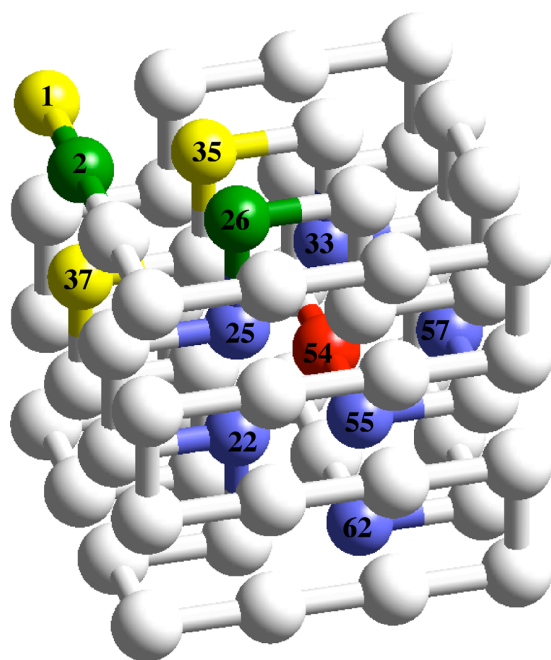


Figure 6